Applied Catalysis B: Environmental 188 (2016) 217–226

Contents lists available at ScienceDirect

Applied Catalysis B: Environmental

journal homepage: www.elsevier.com/locate/apcatb

Electrocatalytic hydrogen evolution reaction on reduced graphene oxide electrode decorated with cobaltphthalocyanine

Duygu Akyüz[a], Bahadır Keskin[b], Utkan Şahintürk[c], Atıf Koca[d,*]

[a] Department of Chemistry, Faculty of Science and Letters, Marmara University, 34722 Göztepe, Istanbul, Turkey
[b] Department of Chemistry, Faculty of Arts&Science, Yildiz Technical University, TR34210 Istanbul, Turkey
[c] Department of Metallurgical and Materials Engineering, Faculty of Chemistry-Metallurgical, Yildiz Technical University, TR34210 Istanbul, Turkey
[d] Department of Chemical Engineering, Engineering Faculty, Marmara University, 34722 Göztepe, Istanbul, Turkey

ARTICLE INFO

Article history:
Received 8 November 2015
Received in revised form 26 January 2016
Accepted 1 February 2016
Available online 3 February 2016

Keywords:
Electrocatalyst
Hydrogen evolution reaction
Phthalocyanine
Click electrochemistry
Graphene Oxide
Reduced graphene oxide

ABSTRACT

Electrocatalytic hydrogen evolution reaction (*HER*) on azido graphene oxide (GO-N_3) and reduced azido graphene oxide (RGO-N_3) electrodes decorated with the cobaltphthalocyanine complex bearing terminal alkyne moieties (***TA-CoPc***) was investigated. GCE/**RGO-N_3** electrode was constructed with the electrochemical reduction of GO-N_3 coated on a glassy carbon electrode. Decoration of GCE/**RGO-N_3** and GCE/**GO-N_3** electrodes were performed with a new electrode modification technique, "click electrochemistry (CEC)", with which ***TA-CoPc*** complex was bonded to azido functional groups of GO-N_3 and RGO-N_3 on the electrodes. The modified GCE/**RGO-N_3**/***TA-CoPc*** and GCE/**GO-N_3**/***TA-CoPc*** electrodes were characterized with square wave voltammetry and electrochemical impedance spectroscopy (EIS), and then tested as heterogeneous electrocatalysts for *HER*. GCE/**RGO-N_3**/***TA-CoPc*** electrode illustrates well electrocatalytic activity by decreasing the over-potential of the bare electrode about 340 mV and increasing the current density of the electrode about 15 fold at low pHs with absolutely high stability and reproducibility.

1. Introduction

Due to the world serious energy problems, the development and realization of alternative energy options become increasingly important. Among the possible options, solar-hydrogen energy systems are among a number of encouraging technologies. Hydrogen is one of the most preferable renewable energy carrier and ideal energy storage, since it has high energy density, and could be easy converted into various available energy forms. One of effective solar-hydrogen conversion approaches is indirect usage of solar energy in electrocatalytic water electrolysis reactions. Highly purified hydrogen can be produced from water electrolysis, but the biggest disadvantage is high-energy consumption of this method [1,2]. In order to reduce the production costs by lowering the overpotential (potential differences between the reversible reduction potential and practical discharge potential) of hydrogen evolution reaction (*HER*), various electrocatalytic materials have been frequently tested as the best solutions [3–6]. A wide variety of functional materials; such as, nickel and cobalt based alloys, MoSx, cobalt clathrochelates, iron hydrogenase, glyoxime and tetraimine complexes [7–10].

Graphene Oxide, strictly two-dimensional material, exhibits exceptionally high crystal and electronic quality, and, despite its short history, has already revealed new potential applications. Within a short time of being available in bulk quantities, graphene oxide, have become highly versatile, inexpensive building blocks for the development of several advanced carbonaceous materials. For example, it is not difficult to imagine the incorporation of a variety of additives into composites of graphene oxide to create novel material compositions [11]. In these novel composites, it is also evident that graphene not only promotes the effective electron transfer [12,13] but also increases the specific surface area through increased dispersion of functional materials. Due to these versatile properties 2-D graphene based functional hybrid nanomaterials have been used for many fields such as, sensors [14,15], transparent conductors [16], purification [17,18], and dye-sensitized solar cells [19,20]. Now a days, GO based materials have been tested as active photocatalysts and photoelectrocatalyst for water splitting reactions [21–24].

GO is an electrically insulating material due to their disrupted sp^2 bonding networks. As-synthesized GO is insulating but controlled deoxidation leads to an electrically and optically active material that is transparent and conducting. Because electrical con-

* Corresponding author.
E-mail address: akoca@marmara.edu.tr (A. Koca).

http://dx.doi.org/10.1016/j.apcatb.2016.02.003
0926-3373/

ductivity can be recovered by restoring the π-network, one of the most important reactions of graphene oxide is its reduction to reduced graphene oxide (RGO) [25]. Thus, RGO is both conductive and has chemically active defect sites making it a promising candidate for the active material in various technological applications, such as, molecular sensors [26,27], catalysts [23,28,29], solar cells [30], and supercapacitors [31,32]. Due to the higher electrically and optically activity of RGO with respect to GO, RGO has been preferred as active photocatalysts [29,33,34] and photoelectrocatalyst [35,36] for the hydrogen production from water splitting reac-

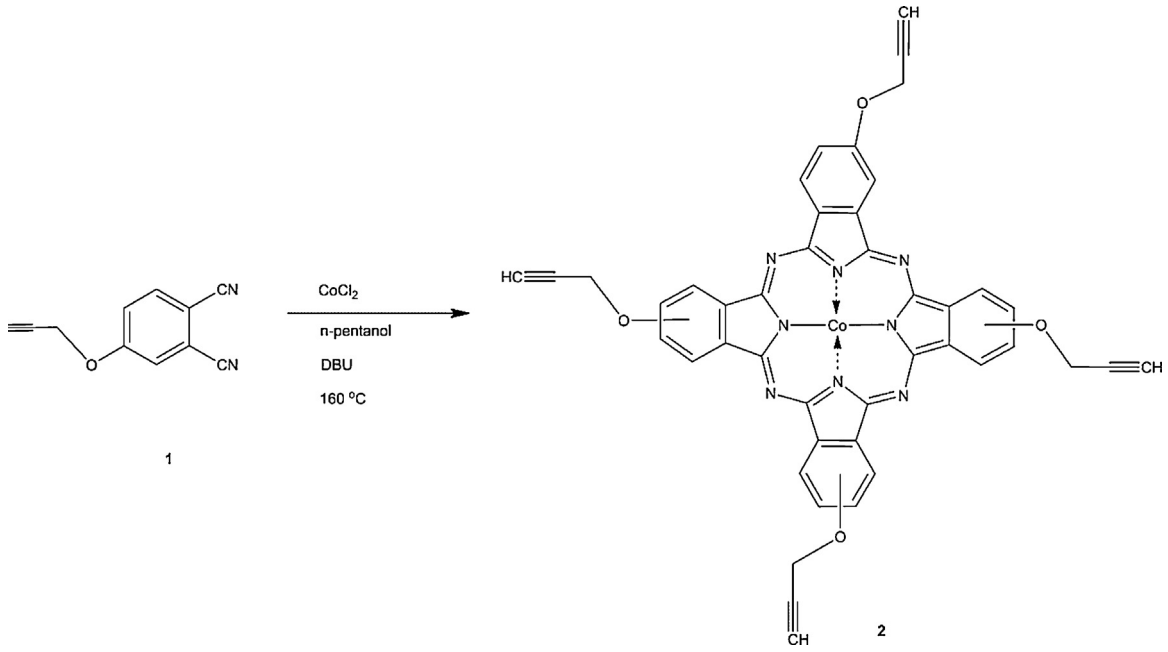

Scheme 1. Synthetic pathways for the phthalonitriles and phthalocyanines (i) $CoCl_2$, DBU, *n*-pentanol, heat, N_2.

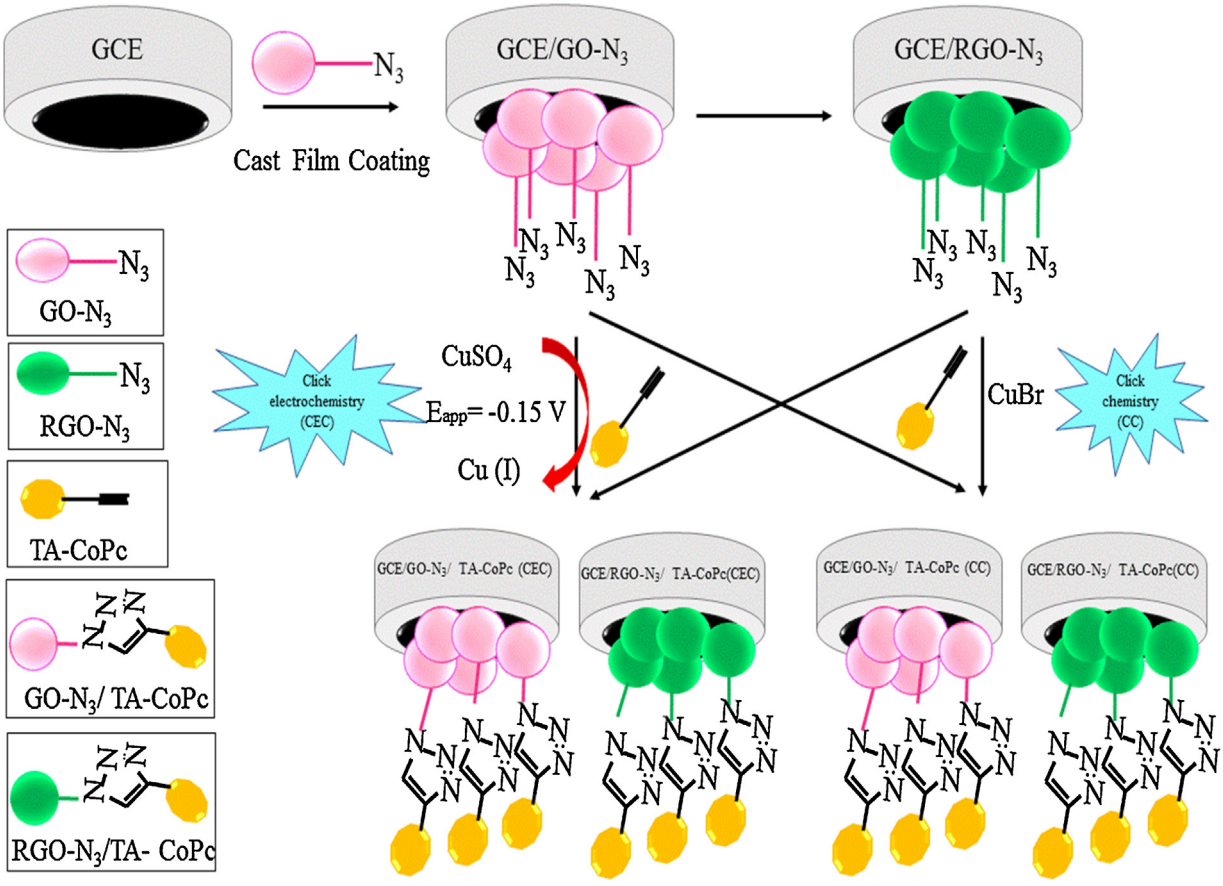

Scheme 2. Electrode modification via the "click chemistry" (CC) and the "click electrochemistry" (CEC) between **GO-N_3**, **RGO-N_3**, and ***TA-CoPc***.

tion. Although GO and RGO were used as active photocatalysts and photoelectrocatalyst for HER and active electrocatalyst for oxygen reduction reactions [37,38], there is only one study on the usage of RGO for the electrocatalytic *HER* from water electrolysis [39]. Tour and coworkers reported that atomic cobalt on nitrogen-doped graphene behaves as active electrocatalyst for hydrogen generation from water instead of platinum [39]. Differently in this paper we used azido functional GO and RGO modified with molecular compounds. Here, we have investigated electrocatalytic activity of GO and RGO based electrodes modified with click electrochemistry between terminal alkyne groups of metallophthalocyanines and azido groups of GO and RGO for the electrocatalytic *HER*.

Generally transition metal complexes of different ligands have been studied in depth as homogeneous and/or heterogeneous electrocatalysts for HER, due to the rich redox properties of such complexes [7–10]. The complexes having metal-based reduction processes observed before *HER* processes generally showed good electrocatalytic activity. It was stated in our previous studies that MPcs having metal-based reduction processes showed higher activities for *HER* [40–42]. Therefore in order to increase electrocatalytic activity of the modified electrodes, GO and RGO were decorated with another active electrocatalyst, terminally alkyne substituted cobalt(II) phthalocyanine (***TA-CoPc***) (Scheme 1). It is well known that especially alkyne substituent systems are particularly important, considering the wide range of functional group interconversions that the triple bond may permit [43,44]. The most common functionality of these system is the click chemistry between alkyne substituent systems and azido functional moieties.For this purpose GO and RGO were functionalized with azido groups and cobalt phthalocyanine was functionalized with terminally alkyne substituents. Then **TA-CoPc** molecules were bonded to the azide groups of GO and RGO with click electrochemistry (CEC) technique and finally **TA-CoPc** decorated GO and RGO based modified glassy carbon electrodes (GCE/**GO-N_3/TA-CoPc** and GCE/**RGO-N_3/TA-CoPc**) were developed. These electrodes have been characterized and tested as the electrocatalyt for *HER*.

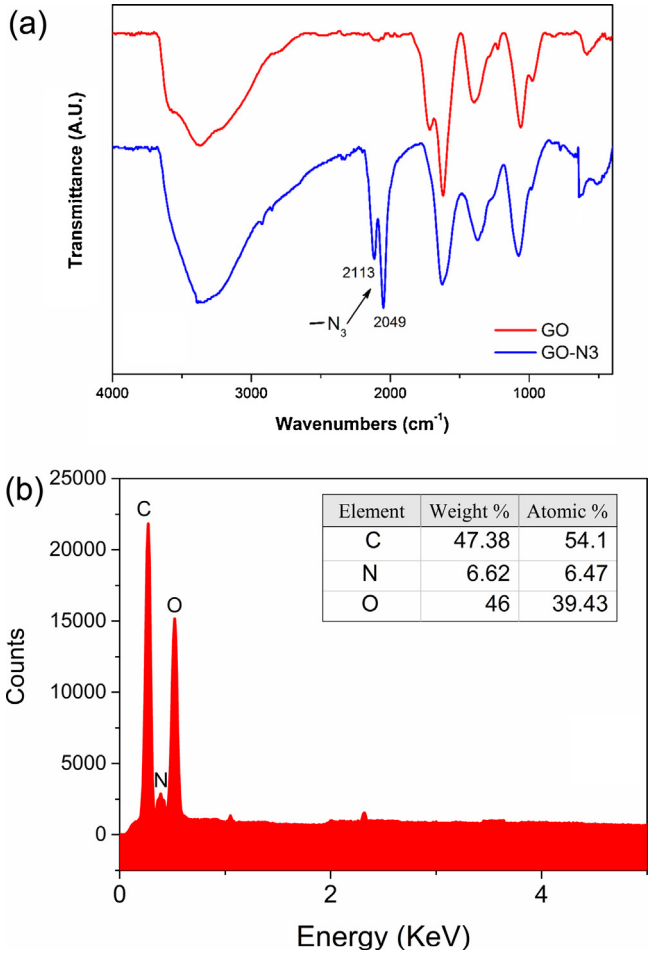

Fig. 1. (a) FTIR spectra of GO and GO-N_3. b) EDX of GO-N_3.

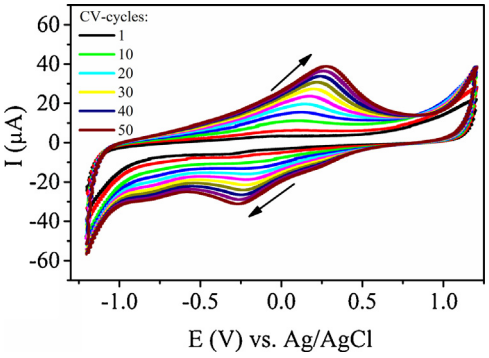

Fig. 2. Repetitive CV responses of **GCE/GO-N_3** electrode at 100 mV s^{-1} scan rate in $LiClO_4/H_2O$ electrolyte system.

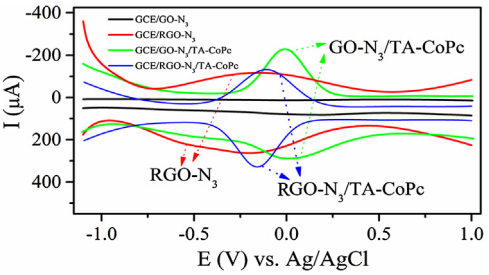

Fig. 3. SWVs of **GCE/GO-N_3**, **GCE/RGO-N_3**, **GCE/GO-N_3/*TA-CoPc***, and **GCE/RGO-N_3/*TA-CoPc*** electrodes recorded at 100 mV s^{-1} scan rate in PBS containing 0.1 M $LiClO_4$.

2. Experimental

2.1. Chemicals and equipment

The experimental studies were carried on with high purity chemicals. Extra pure dimethyl sulfoxide (DMSO), and ultrapure water (≥18 M., Milli-Q, Millipore) were used as solvents. Electrochemical grade tetrabutylammonium perchlorate (TBAP), NaOH, NaCl, H_3PO_4, KH_2PO_4, $LiClO_4$, HCl, and other reagents were purchased from Aldrich and used without further purification. CuBr (Merck Millipore, 8146580050) and $CuSO_4$ (Merck Millipore, 1027910250) were used as received. Graphite powder was purchased from Alfa Aesar (Graphite flake, natural, −325 mesh, 99.8% metal basis), potassium permanganate ($KMnO_4$), sodium nitrate ($NaNO_3$), sulfuric acid (H_2SO_4) were obtained from Merck and hydrogen peroxide (H_2O_2), sodium azide (NaN_3) was from Sigma-Aldrich, and used as received. The phosphate buffer solutions were prepared by using 0.1 $moldm^{-3}$ H_3PO_4, and 0.1 $moldm^{-3}$ KH_2PO_4 and 0.1 mol/dm^3 NaCl. The desired pH was obtained by addition of conjugate acids or 0.1 mol/dm^3 NaOH solution. For CEC techniques; 0.017 g TBAP, 1.80 mg $CuSO_4$, and 0.180 mg ***TA-CoPc*** were dissolved in 2.00 mL DMSO.

Freeze-drying was accomplished on a Christ Alpha 1-2 LD from Martin Christ, Germany. For centrifugation a Nuve NF800 centrifuge was used. The FT-IR spectra were recorded in the 4000–400 cm^{-1} range on Perkin Elmer Spectrum One (ATR sam-

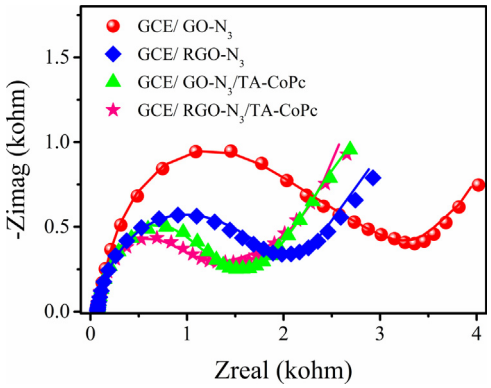

Fig. 4. EISs of **GCE/GO-N_3**, **GCE/RGO-N_3**, **GCE/GO-N_3/*TA-CoPc***, and **GCE/RGO-N_3/*TA-CoPc*** electrodes recorded in $[Fe(CN)_6]^{3-}/[Fe(CN)_6]^{4-}$ aqueous solution.

pling accessory) spectrophotometers. The electronic spectra and absorbance measurements were recorded on Agile 8453 UV–vis spectrophotometer. Proton NMR spectra were recorded on Brucker 250 MHz and Bruker Avance III 500 MHz spectrometers using TMS as internal reference. The mass spectra were acquired on a Bruker Daltonics (Bremen, Germany) MaldiTOF mass spectrometer equipped with an electron spray ionization (ESI) source. The instrument was operated in positive ion mode using an *m/z* range of 50–3000. The capillary voltage of the ion source was set at 6000 V and the capillary exit at 190 V. The nebulizer gas flow was 1 bar and drying gas flow 8 mL/min. Melting points were obtained with a Gallenkamp CAP MPD-350 apparatus in open capillaries. Electrochemical impedance spectroscopy (EIS) measurements of bare and modified electrodes prepared as described above were performed in 1.0×10^{-3} moldm^{-3} $K_3Fe(CN)_6$-$K_4Fe(CN)_6$ aqueous solution under 10 mV AC voltage vs. open circuit potential (open circuit voltage is 0.40 V) in AC frequency range 100 kHz to 0.05 Hz with an 0.40 V excitation DC voltage.

Table 1
Analysis of LSV and CA and CC responses of the bare and modified electrodes during HER measurements.

Electrodes		pHs of the electrolytes			
		3.40	5.60	7.40	10.0
GCE/GO-N_3	ΔE/mV[a]	80	40	48	80
	J (m)/J(b)[b]	2.40	1.7	2.3	2.6
	Q(m)/Q(b)[c]	1.8	1.3	1.7	1.2
	βc (mV dec^{-1})[d]	139	128	136	147
GCE/RGO-N_3	ΔE/mV[a]	130	42	50	110
	J (m)/J(b)[b]	4.1	1.8	3.1	2.7
	Q(m)/Q(b)[c]	3.1	1.6	1.9	1.4
	βc (mV dec^{-1})[d]	91	105	117	106
GCE/GO-N_3/*TA-CoPc*	ΔE/mV[a]	240	300	320	300
	J (m)/J(b)[b]	9.2	7.5	7.2	6.2
	Q(m)/Q(b)[c]	4.8	2.2	2.2	2.5
	βc (mV dec^{-1})[d]	121	138	145	135
GCE/RGO-N_3/*TA-CoPc*	ΔE/mV[a]	340	320	380	310
	J (m)/J(b)[b]	15.0	10.5	13.3	9.3
	Q(m)/Q(b)[c]	6.6	2.7	3.5	4.2
	βc (mV dec^{-1})[d]	131	120	137	140

[a] ΔE/mV: onset potential differences between modified and bare electrodes measured during LSV analysis of HER.
[b] J (m)/J(b): ratio of the current densities of *HER* on modified and bare electrodes recorded with LSVs at the final potentials.
[c] Q(m)/Q(b): ratio of the charge densities of *HER* on modified and bare electrodes recorded with CCs.
[d] βc (mV): Tafel slopes derived from LSVs.

2.2. Synthesis of graphene oxide (GO) and azido graphene oxide (GO-N_3)

GO were prepared according to previously reported procedures with minor changes and characterized by comparing their spectral data to those reported earlier [45,46]. Graphite powder (0.5 g) and sodium nitrate (0.5 g) were placed in concentrated H_2SO_4 (95–98%, 23 mL). The ingredients were mixed in an ice-bath that had been cooled to 0 °C. $KMnO_4$ (3.0 g) was added gradually with stirring and

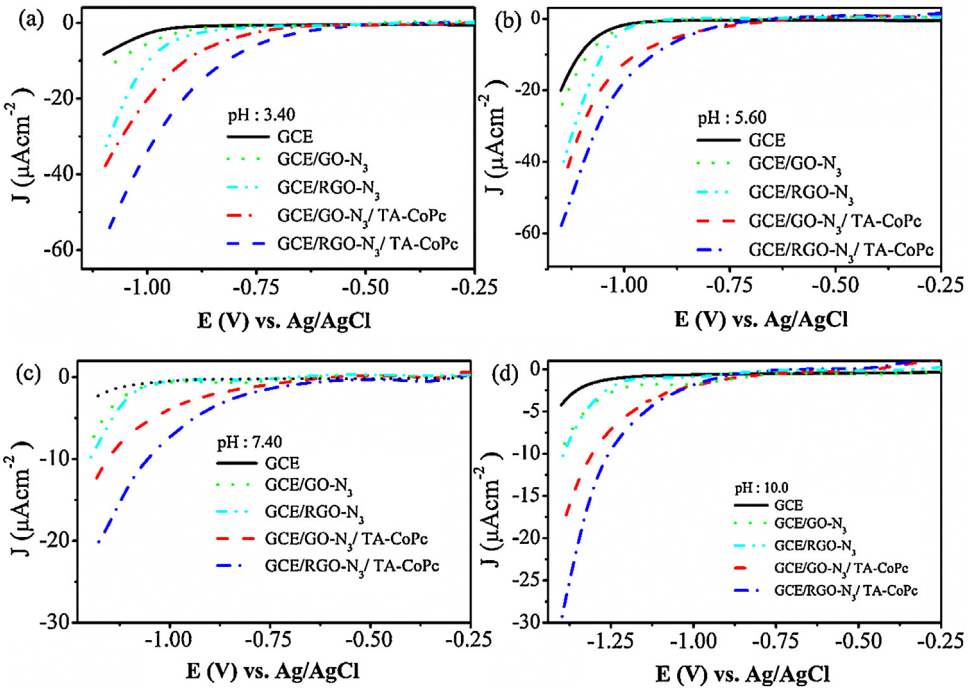

Fig. 5. LSVs of **GCE/GO-N_3**, **GCE/RGO-N_3**, **GCE/GO-N_3/*TA-CoPc***, and **GCE/RGO-N_3/*TA-CoPc*** electrodes recorded at 0.010 mV s^{-1} scan rate with 1000 rpm rotating speed in PBS containing 0.1 M $LiClO_4$. (a) pH 3.40; (b) pH 5.60; (c) pH 7.40; (d) pH 10.00. (pHs of the electrolyte was adjusted with conjugated acid of the buffer solution).

cooling and the mixture was stirred at 35 °C for 60 min. Then, water (40 mL) was added slowly to an increase in temperature to go up and was held with stirring at 90 °C for 30 min. Again, H_2O_2 solution (30%, 3 mL) on ice-water (100 mL) were added until gas evolution was completed. Upon this treatment the suspension turned in color brown to yellow. The suspension was filtered while it was still warm. After washing with water (200 mL). The residue solid was dispersed in water and then centrifuged at 8000 rpm for 15 min two times. Finally, the resultant pure GO was obtained after it was dried at 40 °C for 24 in vacuum. GO was functionalized with sodium azide to product azide-functionalized GO (GO-N_3) by described method and characterized by comparing their spectral data to those reported earlier [47].

2.3. Synthesis of cobalt(II) tetra terminal-alkynyl phthalocyanine (TA-CoPc)

A mixture of compound 4-(prop-2-ynyloxy) phthalonitrile (0.120 g, 0.63 mmol), anhydrous $CoCl_2$ (0.038 g, 0.29 mmol) and 0.20 mL of DBU in dry *n*-pentanol (2 mL) was heated to 155 °C with stirring for 4 h under N_2. The dark green mixture was cooled to room temperature and then was precipitated in hexane. The precipitate was filtered off and washed with hexane and methanol. The crude product was purified by column chromatography on silica gel using eluent THF to afford cobalt phthalocyanine, ***TA-CoPc*** as a blue-green solid. Yield: 0.375 g (75%); m.p. >300 °C. FT-IR (ATR), $\nu_{max}/(cm^{-1})$: 3273 (C═CH), 3076, 3054 (C—H_{arom}), 2954 (C—H_{alip}), 2116 (C═C), 1584, 1430 (C═C_{ar}), 1313 and 1156 (C—O—C). UV/VIS (DMF) λ_{max}/nm (log ε): 669 (4.34), 328 (4.28). Anal. Calc. for $C_{44}H_{24}N_8O_4Co$: C, 67.09; H, 3.07; N, 14.23. Found: C, 66.98; H, 3.01; N, 14.15%. ESI-MS: *m*/*z* Calc.: 787.64; Found: 788.82 $[M+H]^+$.

2.4. Electrode modification

GC working electrodes were modified with GO-N_3 and RGO-N_3 decorated with ***TA-CoPc*** by using click chemistry (CC) and click electrochemistry (CEC) techniques. During these modification processes, ***TA-CoPc*** was bonded to azido sides of GO-N_3 and RGO-N_3 coated on GCE previously. For CC and CEC reactions, following solutions were used.

2.4.1. GCE/GO-N_3 electrode preparation

5.0 mg GO-N_3 were dissolved in 2.0 mL ultra-pure water under ultrasonic bath for 30 min. Then 30 μL the solution was casted on GCE and was dried in vacuum at 70 °C for 20 min. Finally **GCE/GO-N_3** rinsed several times with water and used as the working electrode.

2.4.2. GCE/RGO-N_3 electrode preparation

A Pt wire, and Ag/AgCl separated from the bulk of the solution by a double bridge were used as counter and reference electrodes respectively. $LiClO_4$ in ultra-pure water was the supporting electrolyte at a concentration of 0.10 mol dm^{-3}. Repeating 50 CV cycles between −1.20 V and + 1.20 V in $LiClO_4/H_2O$ electrolyte system were employed to reduce GO-N_3 and to form GCE/RGO-N_3 working electrode. Then **GCE/RGO-N_3** electrode was dried in vacuum at 70 °C for 20 min. Finally **GCE/RGO-N_3** rinsed several times with water and used as the working electrode.

2.4.3. Preparation of GCE/GO-N_3/TA-CoPc and GCE/RGO-N_3/TA-CoPc electrodes with CEC

For the traditional click chemistry (CC), Cu(I) ion (here we used CuBr) is used as catalyst for the reaction between azido and alkyne groups as shown in Scheme 2. For CEC reaction, Cu(I) catalyst was controllably produced at the electrode surface with the chronoamperometry (CA) technique. Cu(I) ions were produced from $CuSO_4$/DMSO solution. It was determined that $CuSO_4$ gave Cu^{II}/Cu^{I} couple at −0.15 V in DMSO, thus CA measurements were performed at −0.15 V in order to produce Cu(I) ions on the electrode surface. CEC was performed in $CuSO_4$, and ***TA-CoPc*** dissolved DMSO solution on GCE/GO-N_3 and GCE/RGO-N_3 working electrodes in three steps. First of all, CV of GCE/GO-N_3 and GCE/RGO-N_3 electrodes were recorded between 0 V and 1.10 V in ***TA-CoPc*** dissolved DMSO solution to determine the electrochemical responses of ***TA-CoPc*** and GO-N_3 and RGO-N_3 in "solution II" before CEC. Then with CA technique, −0.15 V constant potential was applied to GCE/GO-N_3 and GCE/RGO-N_3 working electrodes to generate Cu^{I} ions electrochemically needed for CEC. Time interval of the CA technique was optimized as 10 min. Finally, CV of the working electrode was sequentially recorded between −0.15 V and 1.10 V to determine the electrochemical responses of **GCE/GO-N_3/*TA-CoPc*** and **GCE/RG O-N_3/*TA-CoPc*** electrodes after CEC. The modified electrodes were dried in vacuum at 70 °C for 20 min, and finally used as an electrocatalyst for *HER*.

2.5. Electrochemical measurements

The electrochemical applications and measurements were performed with a potentiostat (GAMRY Instruments, Reference 600Potentiostat/Galvanostat/ZRA) utilizing a three-electrode cell configuration at 25 °C. For cyclic voltammetry (CV) and square wave voltammetry (SWV) measurements, the working electrode was a bare or modified glassy carbon electrode (GCE) with a surface area of 0.071 cm^2 (diameter of the electrodes are 3 mm). For linear sweep voltammetry (LSV), chronoamperometry (CA), and chronocoulometry (CC) measurements, a rotating disk bare or modified GCEs were used as working electrodes at 1000 rpm rotating speed. A Pt wire was used as the counter electrode. Ag/AgCl electrode was employed as the reference electrode and separated from bulk of the solution by a double bridge. High purity N_2 was used to remove dissolved O_2 for at least 15 min prior to each run and to maintain a nitrogen atmosphere over the solution during the measurements.

Electrocatalytic measurements were performed with LSV, CA, and CC techniques. During electrocatalytic measurements, *HER* was analyzed on different working electrodes at different pHs. Aqueous phosphate buffer solution containing 0.1 mol/dm^3 $LiClO_4$ in triple distilled water was employed as supporting electrolyte. To prove the hydrogen evolution, electrolysis at hydrogen discharge potential was performed and evolved gas was analyzed by an Agilent 6890N Gas Chromatography.

3. Result and discussion

3.1. Syntheses and characterizations

Hummers' method is the most common method used for preparing graphene oxide [48], used strong oxidizing mixtures containing concentrated sulfuric acid (H_2SO_4) and oxidizing materials such as potassium permanganate and sodium nitrate. GO powder made from the modified Hummers method, the preparation of GO is described. In contrast to traditional Hummers' method, we prepared the GO increasing the amount of $KMnO_4$, and $NaNO_3$ improves the efficiency of the oxidation process. This modified method provides a greater amount of hydrophilic oxidized graphene material. Moreover, GO produced by our method is more oxidized than that prepared by Hummers' method, when both are reduced in the same chamber with hydrazine hydrate (N_2H_4), reduced graphene oxide produced from modified yield increase. GO was functionalized with sodium azide (NaN_3) to product azide-functionalized GO-N_3 by described method [47]. A dispersion of GO and sodium azide was freeze-dried, due to the reaction does not proceed in solution but only in the solid state during drying of

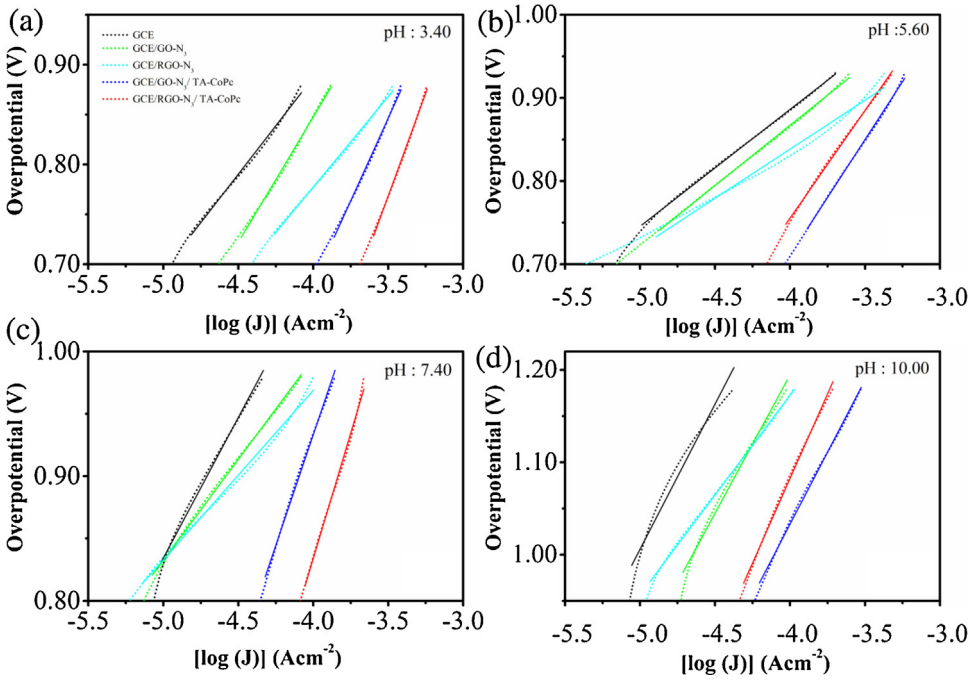

Fig. 6. Tafel plots of **GCE/GO-N$_3$**, **GCE/RGO-N$_3$**, **GCE/GO-N$_3$/*TA-CoPc***, and **GCE/RGO-N$_3$/*TA-CoPc*** electrodes recorded at 0.010 mV s^{-1} scan rate with 1000 rpm rotating speed in PBS containing 0.1 M $LiClO_4$. (a) pH 3.40; (b) pH 5.60; (c) pH 7.40; (d) pH 10.00. (pHs of the electrolyte was adjusted with conjugated acid of the buffer solution).

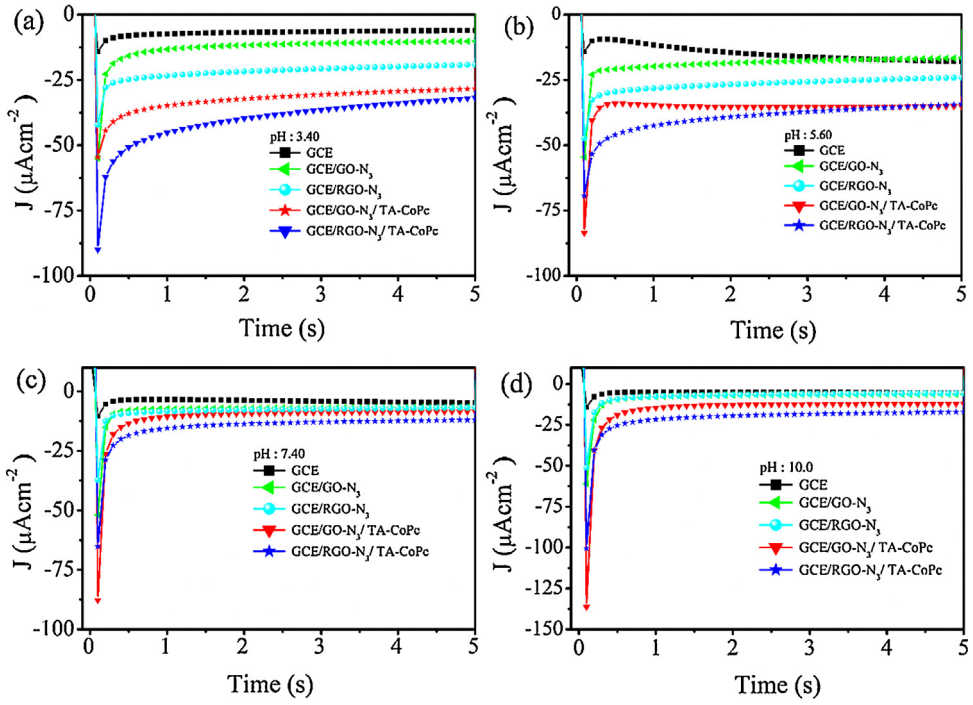

Fig. 7. CAs of **GCE/GO-N$_3$**, **GCE/RGO-N$_3$**, **GCE/GO-N$_3$/*TA-CoPc***, and **GCE/RGO-N$_3$/*TA-CoPc*** electrodes recorded at 0.010 mV s^{-1} scan rate with 1000 rpm rotating speed in PBS containing 0.1 M $LiClO_4$. (a) pH 3.40; (b) pH 5.60; (c) pH 7.40; (d) pH 10.00. (pHs of the electrolyte was adjusted with conjugated acid of the buffer solution).

the dispersion. The reaction was successful, after freeze-drying the material was purified by recurring centrifugation and re-dispersion in water. The final GO-N_3 was hydrolytically stable at room temperature and further proved the azide functionalization with the FTIR absorption at 2049 and 2113 cm^{-1}. GO and GO-N_3 FTIR spectra are compared as shown in Fig. 1a. To give further evidence of the controlled mild functionalization of GO with azide, we used the EDX spectroscopy experiment. The composition of this azide modified structure is confirmed by the SEM-EDX spectroscopy which reveals the presence of peak for N along with carbon and oxygen peaks (Fig. 1b).

The first step in the synthetic procedure of ***TA-CoPc*** was to obtain phthalonitrile derivatives containing terminal alkynyl group. The general route for the synthesis of the new phthalocyanines is shown in Scheme 1. This achieved from reaction of a base catalyzed nucleophilic aromatic nitro displacement of 4-nitrophthalonitrile 2-propyn-1-ol to get prop-2-ynyloxy-substituted derivatives was prepared by literature procedures

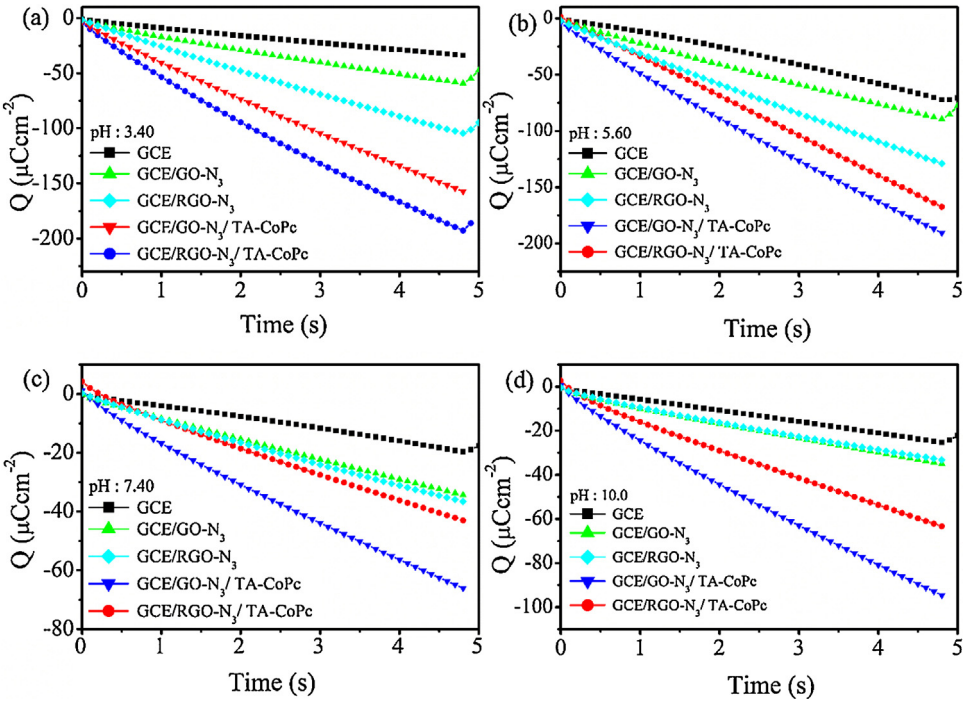

Fig. 8. CCs of **GCE/GO-N$_3$**, **GCE/RGO-N$_3$**, **GCE/GO-N$_3$/*TA-CoPc***, and **GCE/RGO-N$_3$/*TA-CoPc*** electrodes recorded at 0.010 mV s^{-1} scan rate with 1000 rpm rotating speed in PBS containing 0.1 M $LiClO_4$. (a) pH 3.40; (b) pH 5.60; (c) pH 7.40; (d) pH 10.00. (pHs of the electrolyte was adjusted with conjugated acid of the buffer solution).

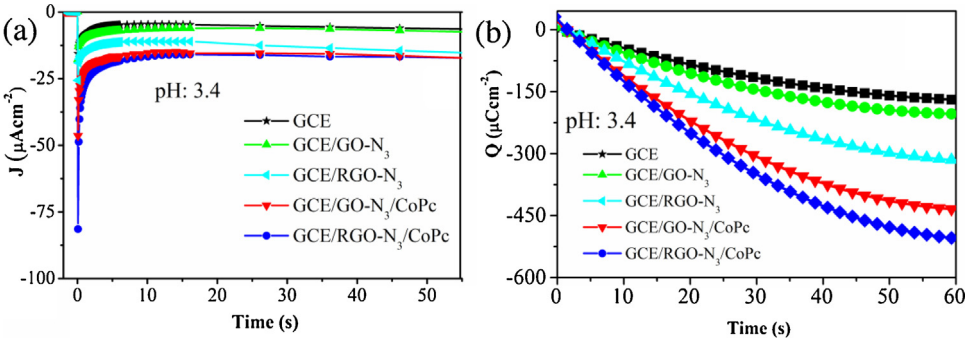

Fig. 9. (a) CA and (b) CCs of **GCE/GO-N$_3$**, **GCE/RGO-N$_3$**, **GCE/GO-N$_3$/*TA-CoPc***, and **GCE/RGO-N$_3$/*TA-CoPc*** electrodes recorded at 0.010 mV s^{-1} scan rate with 1000 rpm rotating speed in PBS containing 0.1 M $LiClO_4$ at pH 3.40 with 60 s excitation.

and characterized by comparing their spectral data to those reported earlier [49]. A template cyclotetramerization of 4-(prop-2-ynyloxy)phthalonitrile was carried out in *n*-pentanol in the presence of metal salts ($CoCl_2$) and DBU as a strong base at ~160 °C under an inert atmosphere for 4 h after purification by column chromatography (eluent THF, SiO_2). The complexes are very soluble in donor solvents (DMSO, THF and DMF), but in soluble in hydrocarbons, and methanol, ethanol. All the compounds were characterized by using many spectroscopic techniques such as FT-IR (Fig. 1), ^{1}H NMR, UV–vis, TLC and elemental analysis. Observation of new bands at 2113 and 2049 cm^{-1} shows binding of $-N_3$ groups to GO. The spectroscopic data of desired products were in accordance with the assigned structures. Elemental analyses agree closely with the values calculated for the compounds.

3.2. Electrode modification and characterization

It is well documented that MPcs bearing redox active metal centers such as, Co^{2+}, Fe^{3+}, and TiO^{2+} behaved as active electrocatalysts for *HER*. GO derivatives were especially studied as active electrocatalyst for oxygen reduction reactions [37,38], however GO-N_3 and RGO-N_3 were firstly used as electrocatalyst for *HER* in this study. Here, we aimed to conduct electrocatalytic activity of **TA-CoPc** with GO-N_3, and RGO-N_3 in order to produce a more active electrocatalyst. Beside the electroactive species, electrode modification technique is one of the most effective parameters on the activity of the catalyst [8,50]. Many different techniques, such as cast film, dip coating, physical adsorption, electrodeposition, electropolymerization, and LB techniques, were reported in the literature for construction of modified electrodes as electrocatalysts of *HER* [51–54]. Here we have designed **GCE/GO-N$_3$/*TA-CoPc*** and **GCE/RGO-N$_3$/*TA-CoPc*** electrodes with CEC. CEC was developed with our research group previously and modified electrodes with CEC were used as active electrocatalyst for HER and selective and sensitive electrochemical pesticide sensors [55,56]. Here, we use CEC technique for the construction of ***TA-CoPc*** decorated GO and RGO based modified electrodes and we investigate electrocatalytic activities of these electrodes for *HER*.

For CEC modification technique, GO was functionalized with azido groups. Azido functionalized GO (GO-N_3) was coated on GCE with cast film technique and **GCE/GO-N$_3$** electrode was constructed. **GCE/GO-N$_3$** electrode was electrochemically reduced to

GCE/RGO-N_3 electrode with repetitive CV technique. GO contains oxygen functional groups, such as epoxides, −OH, and −COOH groups, which make it hydrophilic and disperse in water very well. However, GO is incompatible with most organic species e.g. TA-CoPc. Chemically reduced GO also tends to aggregate or restack irreversibly to form graphite through Van der Waals interactions [57,58]. To avoid this herein, different from the existing chemically reduced GO, we propose a novel method to directly reduce GO-N_3 by using an electrochemical method, which is fast, clean, and nondestructive for controlled modification and reduction of materials [59]. As shown in Fig. 2, observation of the redox couple with increasing peak current as a function of CV cycles indicates the reduction of **GO-N_3** to **RGO-N_3**. Similar results were reported in the literature about the electrochemical reduction of GO to RGO [60–62]. Then both of **GCE/GO-N_3** and **GCE/RGO-N_3** electrodes were decorated with ***TA-CoPc***. During CEC modification reaction, ***TA-CoPc*** was bonded to azide groups on **GCE/GO-N_3** and **GCE/RGO-N_3** electrodes with the reaction between "azide" and terminal alkyne groups of ***TA-CoPc*** with the catalytic aid of Cu(I). Cu(I) ions were electrochemically produced from $CuSO_4$/DMSO solution on the surface of **GCE/GO-N_3** and **GCE/RGO-N_3** electrodes with CA technique at −0.15 V. Cu(I) ions on the surface of **GCE/GO-N_3** and **GCE/RGO-N_3** electrodes catalyzed the click reaction between **RGO-N_3** and terminal alkyne groups of ***TA-CoPc*** and this catalytic reaction provided the formation of **GCE/GO-N_3/*TA-CoPc*** and **GCE/RGO-N_3/*TA-CoPc*** electrodes as given in Scheme 2.

Modified electrodes were characterized with SWV and EIS techniques. Fig. 3 shows SWV responses of GCE, **GCE/GO-N_3/*TA-CoPc*** and **GCE/RGO-N_3/*TA-CoPc*** electrodes in $LiClO_4/H_2O$ electrolyte. While **GCE/GO-N_3** electrode does not give any redox response, **GCE/RGO-N_3** electrode shows a broad redox couple at around 0.20 V **GCE/GO-N_3/*TA-CoPc*** and **GCE/RGO-N_3/*TA-CoPc*** electrodes give $[Co^{II}Pc^{2-}]/[Co^{I}Pc^{2-}]^{1-}$ based redox couple at 0.0 and 0.10 V respectively. These results are in harmony with the CEC reactions of various MPcs reported by our research group [55,56]. Observation of a ***TA-CoPc*** based redox process illustrates binding of ***TA-CoPc*** to the azide groups on **GO-N_3** and **RGO-N_3**.

EIS analyses of the modified electrodes also indicate formation of **GCE/GO-N_3/*TA-CoPc*** and **GCE/RGO-N_3/*TA-CoPc*** electrodes as shown in Fig. 4. Radius of the semicircles of EIS response of **GCE/RGO-N_3** is smaller than that of **GCE/GO-N_3**, which shows increasing the conductivity of the electrode during the reduction of **GO-N_3** to **RGO-N_3**. Binding of ***TA-CoPc*** to **GCE/GO-N_3** and **GCE/RGO-N_3** electrodes also increases the conductivity of the electrodes as shown in Fig. 4. **GCE/RGO-N_3/*TA-CoPc*** electrode has the highest conductivity among the modified electrodes. Consequently, sufficient conductivities and redox activities of **GCE/GO-N_3/*TA-CoPc*** and **GCE/RGO-N_3/*TA-CoPc*** electrodes show usability of these electrodes as heterogeneous electrocatalyst for *HER*. Therefore, electrocatalytic activities of these electrodes for *HER* were examined with different voltammetric and chronoamperometric techniques.

3.3. Electrocatalytic hydrogen evolution reactions

LSV analyses of the bare and modified electrodes were carried out in order to compare catalytic activities of the electrodes (Fig. 5). Fig. 5a illustrates the electrocatalytic responses of the modified electrodes for *HER* at pH 3.4. Onset potential of *HER* (the potential at which the faradic current is observed) on the bare GCE only shifts from −0.98 V to −0.90 V when GCE was coated with GO-N_3. Reduction of GO-N_3 to RGO-N_3 changes the onset potential to −0.85 V. Decoration of **GCE/GO-N_3** and **GCE/RGO-N_3** electrodes decreases the onset potential of HER upto −0.74 V and −0.64 V respectively. These LSV studies show that both of **GCE/GO-N_3/*TA-CoPc*** and **GCE/RGO-N_3/*TA-CoPc*** electrodes efficiently catalyze the proton reduction by the electro-reduced ***TA-CoPc*** species. Catalytic activities of the electrodes changes slightly with increasing pH of the solution. As shown in Fig. 5a, positive potential shifts of *HER* onset potentials and enhancing in the current density of *HER* process indicate electrocatalytic activities of the electrodes at all pH values, however the best results are observed at low pHs [63–67]. With increasing pH, while the current densities decrease, the overpotential decrease on **GCE/RGO-N_3/*TA-CoPc*** electrode reaches to 380 mV at pH 7.40. Over-potential decreases (ΔEo) and current density ratio of *HER* on the modified to the bare electrode (J_m/J_b) are given in Table 1 in order to illustrate the effect of the modification technique and pH of the solution to the electrocatalytic activities of the modified electrodes. The highest catalytic activity was observed on **GCE/RGO-N_3/*TA-CoPc*** electrode at pH 3.40 with respect to the current density decreasing and at pH 7.40 with respect to the overpotential. Over-potentials of **GCE/GO-N_3/*TA-CoPc*** and **GCE/RGO-N_3/*TA-CoPc*** electrodes for *HER* decrease about 240 and 340 mV at pH 3.40 respectively and 320 and 380 mV at pH 7.40. In addition to the decrease in the overpotential, approximately 9 and 15-fold enhancements of the current density of *HER* at pH 3.40 on **GCE/GO-N_3/*TA-CoPc*** and **GCE/RGO-N_3/*TA-CoPc*** electrodes respectively indicate superior catalytic activities of the electrode.

Tafel plots are used to determine mechanism and evaluate the efficiency of the catalytic reaction [68]. During *HER* in acidic media, the initial step involves the reduction of a proton in solution followed by adsorption of intermediate H_{ads} to the electrode surface as follows:

$$H_3O^+ + e^- + EC \rightarrow EC - H_{ads} + H_2O \quad \text{(Volmer reaction)} \tag{1}$$

A Tafel slope of approximately 120 mV dec^{-1} is associated with this reaction step. This is followed by desorption of H_2 by either of the following reactions:

$$EC - H_{ads} + H_3O^+ + e^- \rightarrow EC + H_2 + H_2O \quad \text{(Heyrovsky reaction)} \tag{2}$$

$$EC - H_{ads} + EC - H_{ads} \rightarrow 2EC + H_2 \quad \text{(Tafel reaction)} \tag{3}$$

The latter reaction has a Tafel slope of approximately 30 mV dec^{-1}. The former has a slope of approximately 120 mV dec^{-1}, when surface coverage of H_{ads} is relatively low. It is known that *HER* at a Pt electrode proceeds via the so-called Volmer–Tafel mechanism with a Tafel slope of 30 mV dec^{-1}. **GCE/GO-N_3/*TA-CoPc*** and **GCE/RGO-N_3/*TA-CoPc*** electrodes displayed Tafel slopes of 121 and 131 mV dec^{-1} at pH of 3.40 respectively (Fig. 6). Observation of Tafel slopes around 120 mV dec^{-1} indicate that the *HER* at these electrodes proceeds via Volmer–Heyrovsky, Eqs. (1) and (2) [69,70].

CA and CC analyses of each electrode were carried out in phosphate buffer solution at different pHs in order to illustrate practical usage of the electrodes for *HER*. During CA and CC analyses, current density-time and charge density-time responses of the electrodes were observed (Figs. 7 and 8). The highest current and charge densities were observed on **GCE/RGO-N_3/*TA-CoPc*** with in 5 s constant potential excitation. For long term behavior test, CA and CC measurements are performed with 60 s measurements (Fig. 9) and it is shown that after ca. 5 s, current change reaches to a stead state and does not change significantly. It is well known that amount of the charge passed from a circuit is directly related with the amount of the produced materials at the electrodes according to Faraday Law. Thus, the highest amount of hydrogen gas can be produced on **GCE/RGO-N_3/*TA-CoPc*** compared to the electrodes studied here.

Stability and reproducibility test of the electrodes were also performed. 10 different **GCE/RGO-N_3/*TA-CoPc*** electrodes were modified and their catalytic activities were tested with LSV and CA in phosphate buffer solution at pH 3.40. The onset potentials and charge density of *HER* on these electrode were compared and it was found that onset potentials was only deviated as 2.2% from each other while the current densities of HER only changes as 3.4%

from each other. LSV response of **GCE/RGO-N_3/*TA-CoPc*** electrode was recorded 100 times. The onset potentials of HER did not almost change, while only 8% deviation was observed on the current density after 100 LSVs with respect to the first LSV measurement. When the stabilities of the electrodes were compared with each other, it was found that **GCE/GO-N_3/*TA-CoPc*** significantly enhanced when graphene oxide was reduced to form **GCE/RGO-N_3/*TA-CoPc***.

Finding new active electrocatalysts that decrease the overpotential of HER and increase the efficiency is now an area of great interest. For these purpose, numerous materials were tested each years. Despite the condense researches in this field, the design of new catalysts with high activity and stability in aqueous media at minimal overpotentials with maximum current density is a real challenge. In this paper, we designed a new dual electrocatalytic system which consisted recently studied RGO and CoPc. MPcs were reported active electrocatalysts for many different target species. In our previous studies, ***MPc*** complexes were reported as active homogeneous and heterogeneous HER catalyst. **RGO** and ***TA-CoPc*** decorated **RGO-N_3** are firstly used as *HER* electrocatalyst in this paper. Especially low over-potential and high current density of *HER* on **GCE/RGO-N_3/*TA-CoPc*** is one of the advantage of this modified electrode as highly active heterogeneous catalyst in the electrocatalytic reduction of H^+ to molecular hydrogen.

4. Conclusions

A graphene based HER electrocatalyst (GO) was firstly reported in this paper. For the decoration of GO with TA-CoPc, GO was functionalized with azide groups (GO-N_3). GO-N_3 was coated on a GCE for practical usage as an electrode (**GCE/GO-N_3**). In order to increase the electrocatalytic activity, **GCE/GO-N_3** was reduced to **RGCE/GO-N_3**. Decoration of **GCE/GO-N_3** and **RGCE/GO-N_3** electrodes with another active electrocatalyst, **TA-CoPc** was performed and aimed electrocatalytic modified electrodes (**GCE/GO-N_3/*TA-CoPc*** and **GCE/RGO-N_3/*TA-CoPc***) were produced. TA-CoPc was bounded to the azide active side of **GO-N_3** and **RGO-N_3**. Both of **GCE/GO-N_3/*TA-CoPc*** and **GCE/RGO-N_3/*TA-CoPc*** behave as active electrocatalyst for HER. Overpotential of *HER* decrease as 340 mV at pH 3.40 on **GCE/RGO-N_3/*TA-CoPc*** electrode. Enhancement of the current density of *HER* on as 15-fold with respect to bare GCE was another superiority of the modified electrode. Analyses of Tafel responses of the electrodes show the proceeding of a Volmer–Heyrovsky mechanism during *HER*. LVS and CA analysis illustrates the reasonable stability and reproducibility of **GCE/RGO-N_3/*TA-CoPc*** electrode.

Acknowledgements

This work is supported by The Research Fund of TUBİTAK (Project no: 113M991) and Marmara University (Project no: FEN-C-YLP-080415-0118). Yildiz Technical University (Project No.: 2012-01-02-GEP08).

References

[1] M. Momirlan, T.N. Veziroglu, The properties of hydrogen as fuel tomorrow in sustainable energy system for a cleaner planet, Int. J. Hydrogen Energy 30 (2005) 795–802.
[2] S.S. Penner, Steps toward the hydrogen economy, Energy 31 (2006) 33–43.
[3] N.H. Afgan, A. Veziroglu, M.G. Carvalho, Multi-criteria evaluation of hydrogen system options, Int. J. Hydrogen Energy 32 (2007) 3183–3193.
[4] W. Vielstich, A. Lamm, H.A. Gasteiger, Handbook of Fuel Cells: Fundamentals Technology and Applications. Vol. 1, Fundamentals and Survey of Systems, Wiley, 2003.
[5] W. Hu, Electrocatalytic properties of new electrocatalysts for hydrogen evolution in alkaline water electrolysis, Int. J. Hydrogen Energy 25 (2000) 111–118.
[6] D. Brown, M. Mahmood, A. Turner, S. Hall, P. Fogarty, Low overvoltage electrocatalysts for hydrogen evolving electrodes, Int. J. Hydrogen Energy 7 (1982) 405–410.
[7] S. Losse, J.G. Vos, S. Rau, Catalytic hydrogen production at cobalt centres, Coord. Chem. Rev. 254 (2010) 2492–2504.
[8] K. Zeng, D. Zhang, Recent progress in alkaline water electrolysis for hydrogen production and applications, Prog. Energy Combust. Sci. 36 (2010) 307–326.
[9] W.M. Singh, T. Baine, S. Kudo, S. Tian, X.A.N. Ma, H. Zhou, N.J. DeYonker, T.C. Pham, J.C. Bollinger, D.L. Baker, Electrocatalytic and photocatalytic hydrogen production in aqueous solution by a molecular cobalt complex, Angew. Chem. 124 (2012) 6043–6046.
[10] S. Srinivasan, F.J. Salzano, Prospects for hydrogen production by water electrolysis to be competitive with conventional methods, Int. J. Hydrogen Energy 2 (1977) 53–59.
[11] O.C. Compton, S.T. Nguyen, Graphene oxide, highly reduced graphene oxide, and graphene: versatile building blocks for carbon-based materials, Small 6 (2010) 711–723.
[12] A.K. Geim, K.S. Novoselov, The rise of graphene, Nat. Mater. 6 (2007) 183–191.
[13] A.K. Geim, Graphene: status and prospects, Science 324 (2009) 1530–1534.
[14] Y. Song, K. Qu, C. Zhao, J. Ren, X. Qu, Graphene oxide: intrinsic peroxidase catalytic activity and its application to glucose detection, Adv. Mater. 22 (2010) 2206–2210.
[15] Q. He, H.G. Sudibya, Z. Yin, S. Wu, H. Li, F. Boey, W. Huang, P. Chen, H. Zhang, Centimeter-long and large-scale micropatterns of reduced graphene oxide films: fabrication and sensing applications, Acs Nano 4 (2010) 3201–3208.
[16] H.A. Becerril, J. Mao, Z. Liu, R.M. Stoltenberg, Z. Bao, Y. Chen, Evaluation of solution-processed reduced graphene oxide films as transparent conductors, Acs Nano 2 (2008) 463–470.
[17] T. Sreeprasad, S.M. Maliyekkal, K. Lisha, T. Pradeep, Reduced graphene oxide-metal/metal oxide composites: facile synthesis and application in water purification, J. Hazard. Mater. 186 (2011) 921–931.
[18] S.-T. Yang, Y. Chang, H. Wang, G. Liu, S. Chen, Y. Wang, Y. Liu, A. Cao, Folding/aggregation of graphene oxide and its application in Cu 2+ removal, J. Colloid Interface Sci. 351 (2010) 122–127.
[19] S.R. Kim, M.K. Parvez, M. Chhowalla, UV-reduction of graphene oxide and its application as an interfacial layer to reduce the back-transport reactions in dye-sensitized solar cells, Chem. Phys. Lett. 483 (2009) 124–127.
[20] L. Kavan, J.H. Yum, M. Grätzel, Optically transparent cathode for dye-sensitized solar cells based on graphene nanoplatelets, ACS Nano 5 (2010) 165–172.
[21] J. Hou, Z. Wang, W. Kan, S. Jiao, H. Zhu, R. Kumar, Efficient visible-light-driven photocatalytic hydrogen production using CdS@ TaON core–shell composites coupled with graphene oxide nanosheets, J. Mater. Chem. 22 (2012) 7291–7299.
[22] P. Gao, J. Liu, S. Lee, T. Zhang, D.D. Sun, High quality graphene oxide–CdS–Pt nanocomposites for efficient photocatalytic hydrogen evolution, J. Mater. Chem. 22 (2012) 2292–2298.
[23] J. Zhang, J. Yu, M. Jaroniec, J.R. Gong, Noble metal-free reduced graphene oxide-$Zn_xCd_{1-x}S$ nanocomposite with enhanced solar photocatalytic H2-production performance, Nano Lett. 12 (2012) 4584–4589.
[24] D. Wang, X. Li, J. Chen, X. Tao, Enhanced photoelectrocatalytic activity of reduced graphene oxide/TiO 2 composite films for dye degradation, Chem. Eng. J. 198 (2012) 547–554.
[25] D.R. Dreyer, S. Park, C.W. Bielawski, R.S. Ruoff, The chemistry of graphene oxide, Chem. Soc. Rev. 39 (2010) 228–240.
[26] J.T. Robinson, F.K. Perkins, E.S. Snow, Z. Wei, P.E. Sheehan, Reduced graphene oxide molecular sensors, Nano Lett. 8 (2008) 3137–3140.
[27] G. Lu, L.E. Ocola, J. Chen, Reduced graphene oxide for room-temperature gas sensors, Nanotechnology 20 (2009) 445502.
[28] Y. Li, W. Gao, L. Ci, C. Wang, P.M. Ajayan, Catalytic performance of Pt nanoparticles on reduced graphene oxide for methanol electro-oxidation, Carbon 48 (2010) 1124–1130.
[29] A. Iwase, Y.H. Ng, Y. Ishiguro, A. Kudo, R. Amal, Reduced graphene oxide as a solid-state electron mediator in Z-scheme photocatalytic water splitting under visible light, J. Am. Chem. Soc. 133 (2011) 11054–11057.
[30] Z. Yin, S. Wu, X. Zhou, X. Huang, Q. Zhang, F. Boey, H. Zhang, Electrochemical deposition of ZnO nanorods on transparent reduced graphene oxide electrodes for hybrid solar cells, Small 6 (2010) 307–312.
[31] B. Zhao, P. Liu, Y. Jiang, D. Pan, H. Tao, J. Song, T. Fang, W. Xu, Supercapacitor performances of thermally reduced graphene oxide, J. Power Sources 198 (2012) 423–427.
[32] J. Zhang, X. Zhao, Conducting polymers directly coated on reduced graphene oxide sheets as high-performance supercapacitor electrodes, J. Phys. Chem. C 116 (2012) 5420–5426.
[33] W. Fan, Q. Lai, Q. Zhang, Y. Wang, Nanocomposites of TiO2 and reduced graphene oxide as efficient photocatalysts for hydrogen evolution, J. Phys. Chem. C 115 (2011) 10694–10701.
[34] S. Min, G. Lu, Dye-sensitized reduced graphene oxide photocatalysts for highly efficient visible-light-driven water reduction, J. Phys. Chem. C 115 (2011) 13938–13945.
[35] Y.H. Ng, A. Iwase, A. Kudo, R. Amal, Reducing graphene oxide on a visible-light BiVO4 photocatalyst for an enhanced photoelectrochemical water splitting, J. Phys. Chem Lett. 1 (2010) 2607–2612.
[36] C. Zhai, M. Zhu, Y. Lu, F. Ren, C. Wang, Y. Du, P. Yang, Reduced graphene oxide modified highly ordered TiO 2 nanotube arrays photoelectrode with

enhanced photoelectrocatalytic performance under visible-light irradiation, Phys. Chem. Chem. Phys. 16 (2014) 14800–14807.
[37] Y. Li, Y. Li, E. Zhu, T. McLouth, C.-Y. Chiu, X. Huang, Y. Huang, Stabilization of high-performance oxygen reduction reaction Pt electrocatalyst supported on reduced graphene oxide/carbon black composite, J. Am. Chem. Soc. 134 (2012) 12326–12329.
[38] X.-Y. Yan, X.-L. Tong, Y.-F. Zhang, X.-D. Han, Y.-Y. Wang, G.-Q. Jin, Y. Qin, X.-Y. Guo, Cuprous oxide nanoparticles dispersed on reduced graphene oxide as an efficient electrocatalyst for oxygen reduction reaction, Chem. Commun. 48 (2012) 1892–1894.
[39] H. Fei, J. Dong, M.J. Arellano-Jiménez, G. Ye, N.D. Kim, E.L. Samuel, Z. Peng, Z. Zhu, F. Qin, J. Bao, Atomic cobalt on nitrogen-doped graphene for hydrogen generation, Nat. Commun. 6 (2015).
[40] Ö.A. Osmanbaş, A. Koca, M. Kandaz, F. Karaca, Electrocatalytic activity of phthalocyanines bearing thiophenes for hydrogen production from water, Int. J. Hydrogen Energy 33 (2008) 3281–3288.
[41] A. Koca, A. Kalkan, Z.A. Bayır, Electrocatalytic oxygen reduction and hydrogen evolution reactions on phthalocyanine modified electrodes: electrochemical, in situ spectroelectrochemical, and in situ electrocolorimetric monitoring, Electrochim. Acta 56 (2011) 5513–5525.
[42] A. Koca, M.K. Şener, M.B. Koçak, A. Gül, Investigation of the electrocatalytic activity of metalophthalocyanine complexes for hydrogen production from water, Int. J. Hydrogen Energy 31 (2006) 2211–2216.
[43] G. Bottari, D.D. Díaz, T. Torres, Alkynyl-substituted phthalocyanines: versatile building blocks for molecular materials synthesis, J. Porphyr. Phthalocyanines 10 (2006) 1083–1100.
[44] E.M. García-Frutos, S.M. O'Flaherty, E.M. Maya, G. de la Torre, W. Blau, P. Vázquez, T. Torres, Alkynyl substituted phthalocyanine derivatives as targets for optical limiting, J. Mater. Chem. 13 (2003) 749–753.
[45] M.R. Das, R.K. Sarma, R. Saikia, V.S. Kale, M.V. Shelke, P. Sengupta, Synthesis of silver nanoparticles in an aqueous suspension of graphene oxide sheets and its antimicrobial activity, Colloids Surf. B: Biointerfaces 83 (2011) 16–22.
[46] S. Eigler, S. Enzelberger-Heim, P. Grimm, W. Hofmann, A. Kroener, C. Geworski, J. Röckert, C. Papp, Wet chemical synthesis of graphene, Adv. Mater. 25 (2013) 3583–3587.
[47] S. Eigler, Y. Hu, Y. Ishii, A. Hirsch, Controlled functionalization of graphene oxide with sodium azide, Nanoscale 5 (2013) 12136–12139.
[48] W.S. Hummers Jr., R.E. Offeman, Preparation of graphitic oxide, J. Am. Chem. Soc. 80 (1958), 1339–1339.
[49] D. Wöhrle, O. Tsaryova, A. Semioshkin, D. Gabel, O. Suvorova, Synthesis and photochemical properties of phthalocyanine zinc (II) complexes containing o-carborane units, J. Organomet. Chem. 747 (2013) 98–105.
[50] A.A. Karyakin, E.E. Karyakina, L. Gorton, The electrocatalytic activity of Prussian blue in hydrogen peroxide reduction studied using a wall-jet electrode with continuous flow, J. Electroanal. Chem. 456 (1998) 97–104.
[51] L.A. Berben, J.C. Peters, Hydrogen evolution by cobalt tetraimine catalysts adsorbed on electrode surfaces, Chem. Commun. 46 (2010) 398–400.
[52] M.P.M. Kaninski, V.M. Nikolic, G.S. Tasic, Z.L. Rakocevic, Electrocatalytic activation of Ni electrode for hydrogen production by electrodeposition of Co and V species, Int. J. Hydrogen Energy 34 (2009) 703–709.
[53] L. Liao, S. Wang, J. Xiao, X. Bian, Y. Zhang, M.D. Scanlon, X. Hu, Y. Tang, B. Liu, H.H. Girault, A nanoporous molybdenum carbide nanowire as an electrocatalyst for hydrogen evolution reaction, Energy Environ. Sci. 7 (2014) 387–392.
[54] Y. Zhang, C. Wang, N. Wan, Z. Liu, Z. Mao, Study on a novel manufacturing process of membrane electrode assemblies for solid polymer electrolyte water electrolysis, Electrochem. Commun. 9 (2007) 667–670.
[55] Y. İpek, H. Dincer, A. Koca, Electrode modification based on click electrochemistry between terminal-alkynyl substituted cobalt phthalocyanine and 4-azidoaniline, Sens. Actuators B: Chem. 193 (2014) 830–837.
[56] Y. İpek, H. Dinçer, A. Koca, Selective electrochemical pesticide sensor modified with click electrochemistry between cobaltphthalocyanine and 4-azidoaniline, J. Electrochem. Soc. 161 (2014) B183–B190.
[57] S. Dunn, Hydrogen futures: toward a sustainable energy system, Int. J. Hydrogen Energy 27 (2002) 235–264.
[58] J. Shen, Y. Hu, C. Li, C. Qin, M. Ye, Synthesis of amphiphilic graphene nanoplatelets, Small 5 (2009) 82–85.
[59] S. Thangavel, R. Ramaraj, Polymer membrane stabilized gold nanostructures modified electrode and its application in nitric oxide detection, J. Phys. Chem. C 112 (2008) 19825–19830.
[60] G.K. Ramesha, S. Sampath, Electrochemical reduction of oriented graphene oxide films: an in situ Raman spectroelectrochemical study, J. Phys. Chem. C 113 (2009) 7985–7989.
[61] M. Zhou, Y. Wang, Y. Zhai, J. Zhai, W. Ren, F. Wang, S. Dong, Controlled synthesis of large-area and patterned electrochemically reduced graphene oxide films, Chem. Eur. J. 15 (2009) 6116–6120.
[62] L. Chen, Y. Tang, K. Wang, C. Liu, S. Luo, Direct electrodeposition of reduced graphene oxide on glassy carbon electrode and its electrochemical application, Electrochem. Commun. 13 (2011) 133–137.
[63] O.A. Osmanbas, A. Koca, M. Kandaz, F. Karaca, Electrocatalytic activity of phthalocyanines bearing thiophenes for hydrogen production from water, Int. J. Hydrogen Energy 33 (2008) 3281–3288.
[64] T. Abe, F. Taguchi, H. Imaya, F. Zhao, J. Zhang, M. Kaneko, Highly active electrocatalysis by cobalt tetraphenylporphyrin incorporated in a nafion membrane for proton reduction, Polym. Adv. Technol. 9 (1998) 559–562.
[65] F. Zhao, J. Zhang, T. Abe, D. Wöhrle, M. Kaneko, Electrocatalytic proton reduction by phthalocyanine cobalt derivatives incorporated in poly (4-vinylpyridine-*co*-styrene) Film, J. Mol. Catal. A: Chem. 145 (1999) 245–256.
[66] J. Maruyama, T. Ioroi, T. Hasegawa, T. Mori, Y. Orikasa, Y. Uchimoto, Carbonaceous hydrogen-Evolution catalyst containing cobalt surrounded by a tuned local structure, ChemCatChem 6 (2014) 2197–2200.
[67] A. Koca, Copper phthalocyanine complex as electrocatalyst for hydrogen evolution reaction, Electrochem. Commun. 11 (2009) 838–841.
[68] L. Chen, A. Lasia, Study of the kinetics of hydrogen evolution reaction on nickel-zinc alloy electrodes, J. Electrochem. Soc. 138 (1991) 3321–3328.
[69] M. Bhardwaj, R. Balasubramaniam, Uncoupled non-linear equations method for determining kinetic parameters in case of hydrogen evolution reaction following Volmer–Heyrovsky–Tafel mechanism and Volmer–Heyrovsky mechanism, Int. J. Hydrogen Energy 33 (2008) 2178–2188.
[70] M.T. Koper, Thermodynamic theory of multi-electron transfer reactions: implications for electrocatalysis, J. Electroanal. Chem. 660 (2011) 254–260.